

Study of the effects of Pauli blocking and Pauli non-locality on the optical potential.

M. A. G. Alvarez and N. Alamanos

DSM/DAPNIA/SPhN CEA-Saclay, 91191 Gif-sur-Yvette, France

L. C. Chamon and M. S. Hussein

*Instituto de Física da Universidade de São Paulo,
Caixa Postal 66318, 05315-970 São Paulo, SP, Brazil*

(Dated: November 3, 2018)

Abstract

Elastic scattering angular distributions for systems with reduced mass between 3 and 34 and energies varying between 25 and 120 MeV/nucleon were analyzed. The stable ^4He , its exotic partner ^6He , and the weakly bound $^6,7\text{Li}$ nuclei were included as projectiles in the systematics. Optical model data analyzes were performed with an adjustable factor of normalization included in the imaginary part of the potential. These analyzes indicated a reduction of absorption for systems with small reduced masses that was detected due to the refractive nature of the scattering by light systems.

PACS numbers: 24.10.Ht,25.70.Bc

I. INTRODUCTION

The elastic scattering of light heavy-ions at intermediate energies has clearly demonstrated the sensitivity at large angles to the underlying optical potential through the "appearance" in the angular distribution of Airy oscillations associated with nuclear rainbow scattering [1]. Such studies pin down several aspects of the optical potential, usually constructed through the double-folding procedure. Among these aspects, we mention the degree of non-locality, genuine energy-dependence, the density dependence of the effective nucleon-nucleon G-matrix, etc.

Recently, the elastic scattering of halo-type nuclei, such as ^{11}Li , ^6He , ^{11}Be , ^{19}C , at intermediate energies has been studied. In such cases, due to the low beam intensity, it is rather difficult to cover the Airy region. Thus, at most, one is bound to extract from the small angle, near/far interference, region, information about the strength of the coupling to the break-up channel. The energy dependence associated with non locality of the local equivalent optical potential has a paramount importance in such studies.

In this work, we discuss the elastic scattering of stable, weakly bound and exotic nuclei on a variety of targets, both light and heavy, in order to assess the energy-dependence. For this purpose, we use the São Paulo potential and the Lax interaction discussed in details in Refs. [2, 3, 4]. In section II, we give an account of the optical potential and its energy-dependence. In section III, we present the data analysis. Finally, in section IV, we present a summary and concluding remarks.

II. THE OPTICAL POTENTIAL

Two different phenomena, called Pauli non-locality (PNL) and Pauli blocking (PB), are important to understand the energy-dependence of the optical potential for heavy-ion systems. The PNL arises from quantum exchange effects and has been studied in the context of neutron-nucleus [5], alpha-nucleus [6] and heavy-ion [2, 3, 7, 8, 9, 10, 11, 12, 13, 14, 15, 16] collisions. The nonlocal interaction has been used in the description of the elastic scattering process through an integro-differential equation [2, 3, 5]. It is possible to define a local-equivalent potential which, within the usual framework of the Schroedinger differential equation, reproduces the results of the integro-differential approach [3, 5]. In the case

of heavy-ion systems, the real part of the local-equivalent interaction is associated to the double-folding potential (V_F) through [3]:

$$V_N(R) = V_F(R)e^{-4v^2/c^2} \quad (1)$$

where c is the speed of light and v is the local relative velocity between the two nuclei. This model is known as São Paulo potential. The velocity/energy-dependence of the potential is very important to account for the data from near-barrier to intermediate energies [2, 3, 7, 8, 9, 10, 11, 12, 13, 14, 15]. Eq. (1) describes the effect of the PNL on the real part of the potential, but the local-equivalent potential that arises from the solution of the corresponding integro-differential equation indicates that the exchange correlation also affects the imaginary part of the optical potential [2].

Another model used in the analyzes of elastic scattering data is the Lax interaction [4], which is the optical limit of the Glauber high-energy approximation [17]. The Lax interaction is essentially a zero range double-folding potential used for both the real and imaginary parts of the optical potential. Similar to the São Paulo potential, the Lax interaction is also dependent on the nuclear densities and may be expressed in terms of the relative velocity between the two nuclei. The imaginary part of the Lax interaction is thus written as:

$$W(R) = -\frac{1}{2}\hbar v \int \sigma_T^{NN}(v)\rho_1(\vec{r})\rho_2(\vec{r} - \vec{R}) d\vec{r} \quad (2)$$

where $\sigma_T^{NN}(v)$ is an energy-dependent spin-isospin-averaged total nucleon-nucleon cross-section. Eq. (2) has been derived from multiple-scattering theories and should be valid for stable (non-exotic) nuclei at high energies. For lower energies, Eq. (2) must be corrected in order to take into account the closure of the phase space due to the Pauli exclusion principle. This phenomenon, known as Pauli blocking (PB), can be simulated in Eq. (2) by introducing a further dependence of σ_T^{NN} on the densities of the nuclei [4]. Usually, the PB is expected to be essential at small internuclear distances due to the corresponding large overlap of the nuclei. Since the PB can distort significantly the densities in the overlap region, it should affect both the real and imaginary parts of the optical potential.

In this work, we have assumed these two semi-phenomenological models for the real (Eq. 1) and imaginary (Eq. 2) parts of the optical potential. We have analyzed several elastic scattering angular distributions for systems with reduced mass between 3 and 34. As extensively discussed in Ref. [3], Eq. (1) can be used in several different frameworks that

provide very similar results in data analyzes. In the present work, we use Eq. (1) within the zero-range approach for the effective nucleon-nucleon interaction ($v_{nn}(\vec{r}) = V_0\delta(\vec{r})$) with the matter densities assumed in the folding calculations (see [3]). This approach is equivalent [3] to the more usual procedure of using the M3Y nucleon-nucleon interaction with the nucleon densities of the nuclei. For σ_T^{NN} in Eq. (2), we have interpolated values from the corresponding experimental results of Ref. [18].

III. DATA ANALYSIS

Table 1 presents all systems that have been analyzed in the present work. The data have been obtained from Refs. [19, 20, 21, 22, 23, 24, 25, 26, 27]. Eqs. (1) and (2) involve the folding of the nuclear densities. In an earlier paper [3], we presented an extensive systematics of heavy-ion densities. In that work, the Fermi distribution was assumed to describe the densities. The systematics indicates that the radii of the matter distributions are well represented by:

$$R_0 = 1.31A^{1/3} - 0.84 \text{ fm.} \quad (3)$$

where A is the number of nucleons of the nucleus. The densities present an average diffuseness value of $a = 0.56$ fm. Owing to specific nuclear structure effects (single particle and/or collective), the parameters R_0 and a show small variations around the corresponding average values throughout the periodic table. In the present work, we have assumed Eq. (3) for all nuclei and allowed a to vary around its average value in order to obtain the best data fits. The only exception is the ${}^4\text{He}$ nucleus for which the shape of the corresponding matter density was assumed to be similar to the charge density obtained from electron scattering experiments [28]. Of course, the use of a Fermi-type density is not well justified for light, both stable and unstable, nuclei. However, we decided to use this universal form in order to assess the adequacy and limitations of our model. The values obtained for the diffuseness of the nuclei are shown in Table 2. In a consistent manner, these values present very small variations around the average value obtained in the previous systematics: $a = 0.56$ fm. We emphasize the much greater value obtained for the diffuseness of the exotic ${}^6\text{He}$ in comparison with its partner ${}^4\text{He}$. Indeed, the diffuseness of the ${}^6\text{He}$ is comparable with the values obtained for heavy-ions. Similar results have already been observed in other works [13, 14]. Table 2 also presents the root-mean-square (RMS) radii for the matter densities

and for charge distributions extracted from electron scattering experiments [28]. The RMS radii for the matter densities agree with the values for charge distributions within about 5%, except for ^{12}C where a difference of 10% was found.

For the imaginary part of the optical potential we have adopted Eq. (2), without PB, multiplied by a factor of normalization N_I . The corresponding predictions for some elastic scattering angular distributions are shown in Figs. (1-3). In these figures, the dashed lines represent the predictions with $N_I = 1$ while the solid ones correspond to the results obtained considering N_I as a free parameter.

The best fit values obtained for N_I are presented in Table 1 and Fig. 4. A strong reduction of absorption is observed for systems with small reduced mass. As already commented in section I, PNL and PB affect both real and imaginary parts of the optical potential. The detected reduction of absorption could partially arise from the effect of the PB. In order to illustrate this point, Fig. (5 - Bottom) shows $W(R)$ obtained from Eq. (2), for the $^{12}\text{C} + ^{12}\text{C}$ system in two different energies, with (solid lines) and without (dashed lines) including the effect of PB. The calculation of $W(R)$ with PB was performed considering a density-dependent nucleon-nucleon total cross section according Refs. [4, 19]. Clearly, the blocking reduces $W(R)$ in an internal region of distances and almost no effect is observed in the surface region. This behavior is connected with the large overlap of the densities for small distances that makes the blocking very effective. In Fig. (5 - Top) we show the results of a notch test, where we have included a spline with Gaussian shape in the imaginary potential and calculated the variation of the chi-square as a function of the position of this perturbation. This test has the purpose of determining the region of sensitivity that is relevant for the elastic scattering process. Just as a guide, the position of the s-wave barrier radius is also indicated in the same figure. In the region of sensitivity, the imaginary potential with PB is in average less intense than the result without blocking. This fact probably is connected with the value $N_I \approx 0.6$ obtained for the $^{12}\text{C} + ^{12}\text{C}$ system. Still in Fig. (5) one can observe that the region of sensitivity is more internal for the higher energy. However, the difference between $W(R)$ with and without blocking is smaller for the higher energy. Probably, these two effects cancel each other and one obtains approximately the same N_I value for the two energies (see Table 1). In Fig. (6) we present the reaction cross sections for the $^{12}\text{C} + ^{12}\text{C}$ system in a very wide energy range (from Refs. [23, 29, 30, 31, 32, 33, 34]). The lines represent the predictions obtained with $N_I = 1$ and $N_I = 0.6$, where the smaller

value was obtained from the elastic scattering data fits. Clearly the value $N_I = 0.6$ also provides a better reproduction of the reaction data in the energy region studied in this work: $25 \leq E \leq 120$ MeV/nucleon that corresponds to $300 \leq E_{Lab} \leq 1440$ MeV for $^{12}\text{C} + ^{12}\text{C}$.

In Fig. (7), we present the notch test for systems with different reduced masses, but for approximately the same bombarding energy. Again as a guide, the positions of the corresponding s-wave barrier radii are indicated in the figure. For the heaviest system, the region of sensitivity is close to the barrier radius and therefore it is in the surface region. The lighter systems present sensitivity regions much more internal in comparison with the corresponding barrier radii. In fact, it is well known that the scattering between light heavy-ions probes more efficiently the internal internuclear distance region [1] and the present results of the notch test just confirms this point. Thus, the simple approach of using Eqs. (1) and (2), with $N_I = 1$, fails for lighter systems that are sensitive to inner distances. The discussion about Fig. 5 clearly shows that the effect of PB on the imaginary part of the potential should be partially responsible by this behavior of light systems, but the present analysis can not discern if such behavior is also connected with effects of PNL on the imaginary part and/or even of PB on the real part of the optical potential. On the other hand, considering our results for heavier systems, the analysis clearly indicates that the surface region of the optical potential is well represented by Eq. (1), real part that includes the PNL effect, and Eq. (2), imaginary part without the PB effect.

In order to check the consistency between the present and earlier works, we have calculated the volume integral of the real part of the potential, Eq. 4, and the reaction cross sections that are connected with the absorptive part of the potential.

$$J_R = \frac{4\pi}{A_1 A_2} \int V(R) R^2 dR \quad (4)$$

The values obtained for J_R and σ_R (see Table 1) are similar to those of earlier works (from Refs. [19, 20, 21, 22, 23, 25, 27, 35, 36, 37, 38, 39, 40, 41]). In the present systematics we have included the weakly bound $^{6,7}\text{Li}$ nuclei and also the exotic ^6He . In some works, due to the break-up process or effects of the halo, these projectiles have been pointed out as responsible by a different behavior in comparison with nuclear reactions involving only normal stable nuclei. In fact, our systematics for N_I also indicates a slightly greater absorption for systems involving $^{6,7}\text{Li}$ in comparison with other systems with similar reduced masses (see Fig. 4). On the other hand, as already commented, the diffuseness obtained in this work for ^6He is

much greater than the value extracted for ${}^4\text{He}$ from electron scattering experiments.

IV. SUMMARY AND CONCLUSIONS

In summary, we have analyzed elastic scattering angular distributions for several systems. The real part of the optical potential was assumed to be energy-dependent due to the PNL that arises from quantum exchange effects. For the imaginary part, we have adopted the Lax interaction that also presents an energy-dependence very well established and connected with the total nucleon-nucleon cross section. In the imaginary part, we have also considered a factor of normalization with the aim of simulating the effect of PB, which arises from the exclusion principle and prevent scattered nucleons to occupy filled states. The notch test indicated that lighter systems present greater sensitivity to the internal region of internuclear distances, where PB is expected to be essential due to the large overlap of the nuclei. For heavier systems it was possible to obtain a good data description with $N_I = 1$. This result indicates that, in the surface region, the PNL and PB does not significantly affect the imaginary part of the potential, while Eq. (1) correctly describes the PNL effect on the real part. For lighter systems, however, reasonable accounts of the data were obtained only considering N_I as a free parameter. This result is compatible with the expected reduction of the absorption due to PB and also with the fact that light nuclei have a smaller density of states. The present analysis, however, can not discern if such behavior is also connected with effects of PNL on the imaginary part and/or even of PB on the real part of the optical potential.

Acknowledgments

This work was partially supported by Financiadora de Estudos e Projetos (FINEP), Fundação de Amparo à Pesquisa do Estado de São Paulo (FAPESP), and Conselho Nacional de Desenvolvimento Científico e Tecnológico (CNPq).

[1] M. E. Brandan and G. R. Satchler, Phys. Rep. **285** (1997) 143.

- [2] L. C. Chamon, D. Pereira, M. S. Hussein, M. A. Candido Ribeiro and D. Galetti, *Phys. Rev. Lett.* **79** (1997) 5218.
- [3] L. C. Chamon, B. V. Carlson, L. R. Gasques, D. Pereira, C. De Conti, M. A. G. Alvarez, M. S. Hussein, M. A. Candido Ribeiro, E. S. Rossi Jr. and C. P. Silva, *Phys. Rev. C* **66** (2002) 014610.
- [4] M. S. Hussein, R. A. Rego and C. A. Bertulani, *Phys. Rep.* **201** (1991) 279.
- [5] F. Perey and B. Buck, *Nucl. Phys.* **32** (1962) 253.
- [6] D. F. Jackson and R. C. Johnson, *Phys. Lett.* **B49** (1974) 249.
- [7] M. A. Candido Ribeiro, L. C. Chamon, D. Pereira, M. S. Hussein and D. Galetti, *Phys.Rev.Lett.* **78** (1997) 3270.
- [8] L. C. Chamon, D. Pereira and M. S. Hussein, *Phys. Rev. C* **58** (1998) 576.
- [9] M. A. G. Alvarez, L. C. Chamon, D. Pereira, E. S. Rossi Jr., C. P. Silva, L. R. Gasques, H. Dias and M. O. Roos, *Nucl. Phys.* **A656** (1999) 187.
- [10] L. R. Gasques, L. C. Chamon, C. P. Silva, D. Pereira, M. A. G. Alvarez, E. S. Rossi Jr., V. P. Likhachev, B. V. Carlson and C. De Conti, *Phys. Rev.* **C65** (2002) 044314.
- [11] M. A. G. Alvarez et al., *Phys. Rev.* **C65** (2002) 014602.
- [12] E. S. Rossi Jr., D. Pereira, L. C. Chamon, M. A. G. Alvarez, L. R. Gasques, J. Lubian, B. V. Carlson and C. De Conti, *Nucl. Phys.* **A707** (2002) 325.
- [13] L. R. Gasques, L. C. Chamon, D. Pereira, M. A. G. Alvarez, E. S. Rossi Jr., C. P. Silva, G. P. A. Nobre and B. V. Carlson, *Phys. Rev.* **C67** (2003) 067603.
- [14] L. R. Gasques et al, *Phys. Rev.* **C67** (2003) 024602.
- [15] M. A. G. Alvarez, L. C. Chamon, M. S. Hussein, D. Pereira, E. S. Rossi Jr. and C. P. Silva, *Nucl. Phys.* **A723** (2003) 93.
- [16] L. R. Gasques, L. C. Chamon, D. Pereira, M. A. G. Alvarez, E. S. Rossi Jr., C. P. Silva and B. V. Carlson, *Phys. Rev C* **69** (2004) 034603.
- [17] R. J. Glauber, W. E. Brittin, L. G. Dunhan (Eds.), *Lectures in Theoretical Physics*, **Vol. 1**, Wiley-Interscience, New York, 1959, p. 315; R. J. Glauber, in: G. Alexander (Ed.), *High Energy Physics and Nuclear Structure*, Wiley, New York, 1967, p. 311; R. J. Glauber *High Energy Physics and Nuclear Structure*, Plenum, New York, 1970, p.207.
- [18] Wilmot N. Hess, *Rev. Mod. Phys.* **30** (1958) 368.
- [19] J.Y. Hostachy, M. Buerned, J. Chauvin, D. Lebrun, Ph. Martin, J. C. Lugol, L. Papineau,

- P. Roussel, N. Alamanos, J. Arvieux and C. Cerruti, Nucl. Phys. **A490** (1988) 441.
- [20] M. E. Brandan, H. Chehime and K. W. Mc Voy, Phys. Rev. C **55**, 1353 (1997).
- [21] V. Lapoux, et al., Phys. Rev. C **66** (2002) 034608.
- [22] A. Nadasen et al, Phys. Rev. C **52** (1995) 1894.
- [23] C. C. Sahm, T. Murakami, J. G. Cramer, A. J. Lazzarini, D. D. Leach, D. R. Tieger, R. A. Loveman, W. G. Lynch, M. B. Tsang and J. Van der Plicht, Phys. Rev. C **34** (1986) 2165.
- [24] Y. T. Oganessian, Y. E. Penionzhkevich, V. I. Man'Ko and V. N. Polyansky, Nucl. Phys. **A303** (1978) 259.
- [25] P. Roussel-Chomaz, N. Alamanos, F. Auger, J. Barrette, B. Berthier, B. Fernandez, L. Papineau, Nucl. Phys. **A477** (1988) 345.
- [26] C. Olmer, M. Mermaz, M. Buenerd, C. K. Gelbke, D. L. Hendrie, J. Mahoney, D. K. Scott, M. H. Macfarlane, S. C. Pieper, Phys. Rev. **C18** (1978) 205.
- [27] J. Albinski, A. Budzanowski, H. Dabrowski, Z. Rogalska, S. Wiktor, H. Rebel, D. K. Srivastava, C. Alderliesten, J. Bojowald, W. Oelert, C. Mayer-Boricke and P. Turek, Nucl. Phys. **A445** (1995) 477.
- [28] H. De Vries, C. W. De Jager and C. De Vries, Atomic Data and Nucl. Data Tables **36** (1987) 495.
- [29] C. Perrin, S. Kox, N. Longequeue, J. B. Viano, M. Buenerd, R. Cherkaoui, A. J. Cole, A. Gamp, J. Menet, R. Ost, R. Bertholet, C. Guet and J. Pinston, Phys. Rev. Lett. **49** (1982) 1905.
- [30] A. J. Cole, W. D. M. Rae, M. E. Brandan, A. Dacal, B. G. Harvey, R. Legrain, M. J. Murphy and R. G. Stokstad, Phys. Rev. Lett. **47** (1981) 1705.
- [31] S. Kox, A. Gamp, R. Cherkaoui, A. J. Cole, N. Longequeue, J. Menet, C. Perin and J. B. Viano, Nucl. Phys. **A420** (1984) 162.
- [32] S. Kox et al, Phys. Rev. C **35** (1987) 1678.
- [33] H. G. Bohlen, M. R. Clover, G. Ingold, H. Lettan, W. von Oertzen, Z. Phys. **A308** (1982) 121.
- [34] M. Buenerd, A. Lounis, J. Chauvin, D. Lebrun, P. Martin, G. Duhamel, J. C. Gondrand, P. de Saintgnon, Nucl. Phys. **A424** (1994) 313.
- [35] A. A. Ogloblin et al, Phys. Rev. **C62** (2000) 44601 .
- [36] M. H. Cha, and Y. J. Kim, Phys. Rev. **C51** (1995) 212.

- [37] D. T. Khoa, G. R. Satchler, and W von Oertzen, Phys. Rev. **C51** (1995) 2069.
- [38] D. T. Khoa, W von Oertzen, and H. G. Bohlen, Phys. Rev. **C49**, (1994) 1652.
- [39] D. T. Khoa and G. R. Satchler, Nucl. Phys. **A668** (2000) 3.
- [40] M. El-Azab Farid and M. A. Hassanain, Nucl. Phys. **A678** (2000) 39.
- [41] D. T. Khoa, G. R. Satchler, and W von Oertzen, Phys. Rev. **C56** (1997) 954.

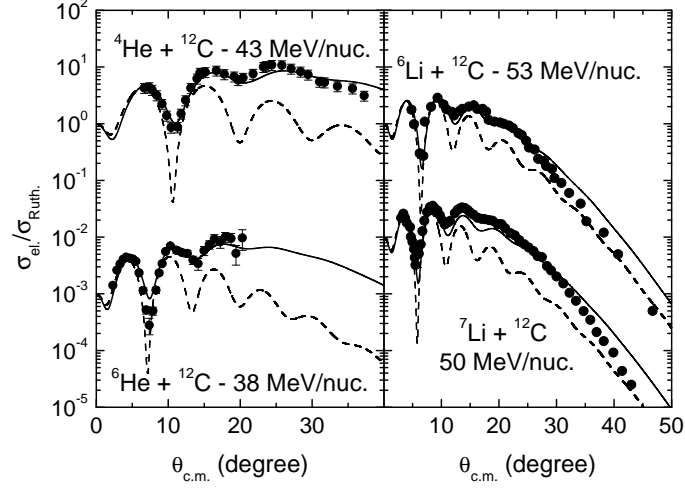


FIG. 1: Elastic scattering angular distributions for the ${}^4,6\text{He}, {}^6,7\text{Li} + {}^{12}\text{C}$ systems. The lines correspond to optical model predictions with (solid lines) or without (dashed lines) including a factor of normalization in the imaginary part of the optical potential.

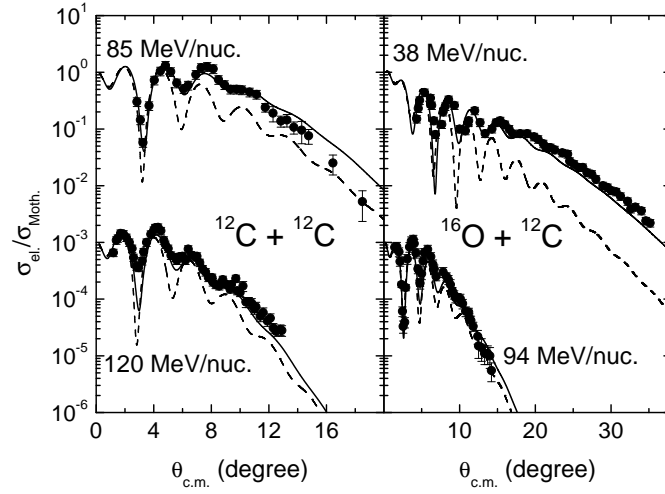


FIG. 2: The same as Fig. 1, for the ${}^{12}\text{C}, {}^{16}\text{O} + {}^{12}\text{C}$ systems.

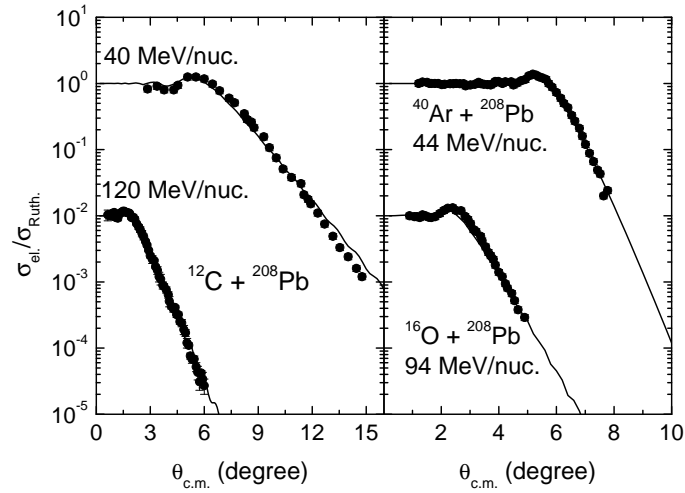


FIG. 3: The same as Fig. 1, for the ^{12}C , ^{16}O , $^{40}\text{Ar} + ^{208}\text{Pb}$ systems.

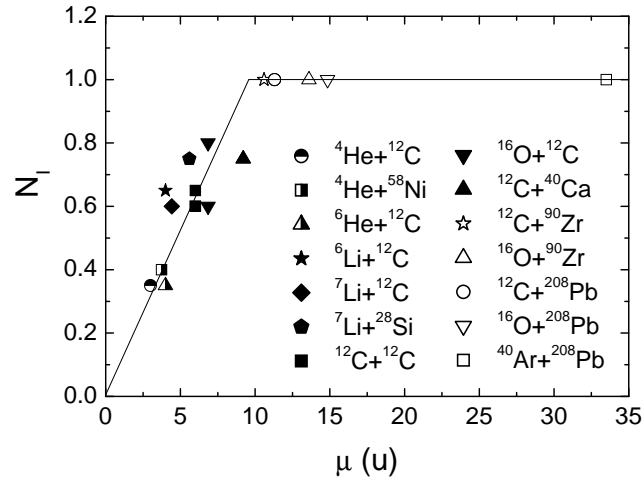


FIG. 4: The factor of normalization of the imaginary part of the potential as a function of the reduced mass of the system. The solid lines are just guides.

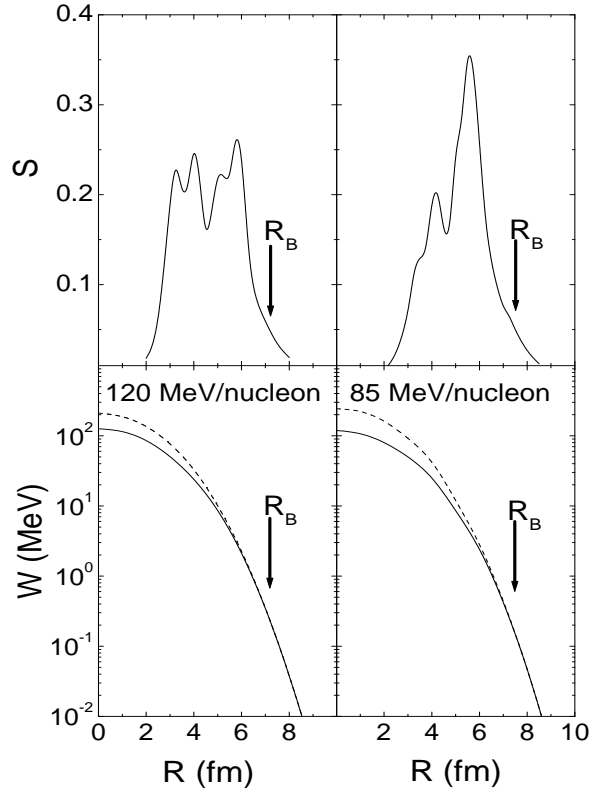


FIG. 5: Bottom - The imaginary part of the optical potential with (solid lines) or without (dashed lines) including the effect of Pauli blocking, for the $^{12}\text{C} + ^{12}\text{C}$ system in two different bombarding energies. The arrows indicate the positions of the s-wave barrier radii. Top - The results of the notch test corresponding to these two elastic scattering angular distributions. The quantity S represents the relative difference between the chi-squares obtained with and without a Gaussian perturbation, centered in R , in the imaginary part of the potential.

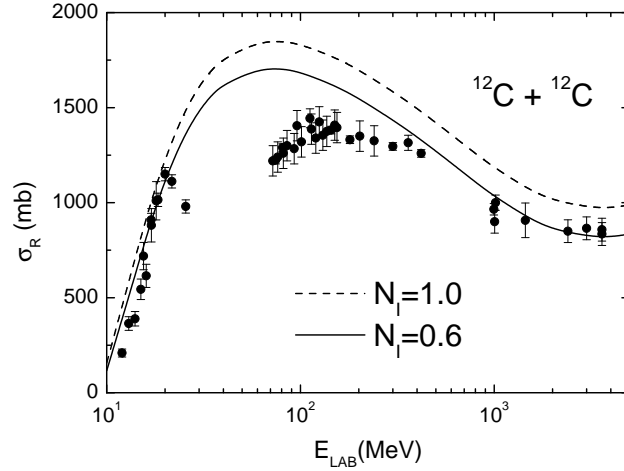


FIG. 6: The reaction cross section as a function of the energy for the $^{12}\text{C} + ^{12}\text{C}$ system. The lines represent the results obtained from optical model calculations, with different factors of normalization for the imaginary part of the potential.

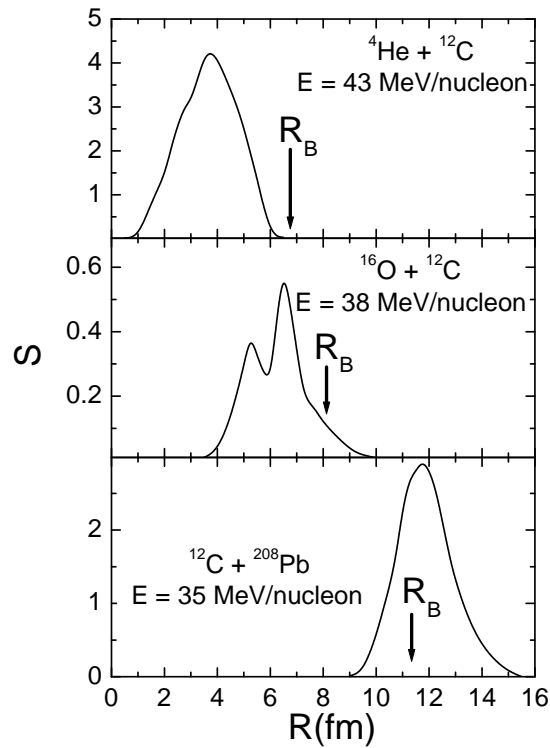


FIG. 7: The regions of sensitivity for three different systems as determined by the notch test. The arrows indicate the positions of the s-wave barrier radii.

TABLE I: Systems that have been analyzed in the present work, their corresponding reduced masses, and the energies (in MeV/nucleon units) of the respective elastic scattering angular distributions. The table also presents the best fit values for the factor of normalization N_I of the imaginary part of the optical potential, the volume integrals (J_R in MeV fm³ units) for the real part of the optical potential, and the reaction cross sections (σ_R in mb units) obtained in the present work (PW). For purpose of comparison, the ranges for J_R and σ_R obtained in earlier works (EW - see refs. in the text) are also included in the table.

Proj.	Target	E	$\mu(u)$	N_I	J_R PW	J_R EW	σ_R PW	σ_R EW
⁴ He	¹² C	43	3.00	0.35	282	244-277	659	718
⁴ He	⁵⁸ Ni	43	3.74	0.40	274	251-287	1437	
⁶ He	¹² C	38	4.00	0.35	299		923	1092-1179
⁶ Li	¹² C	53	4.00	0.65	267	239-296	964	904-1184
⁷ Li	¹² C	50	4.42	0.60	271	260-288	1003	969-1021
⁷ Li	²⁸ Si	50	5.60	0.75	267	227-257	1491	1462-1666
¹² C	¹² C	85	6.00	0.60	206	185	1061	1000
¹² C	¹² C	120	6.00	0.65	156	140	979	907
¹⁶ O	¹² C	38	6.85	0.60	296	225-233	1463	1374
¹⁶ O	¹² C	94	6.85	0.80	191	156	1227	1136
¹² C	⁴⁰ Ca	25	9.20	0.75	323		2209	2030
¹² C	⁹⁰ Zr	25	10.60	1.00	320		2993	2415
¹² C	⁹⁰ Zr	35	10.60	1.00	297		2939	2840
¹² C	²⁰⁸ Pb	25	11.30	1.00	320		3820	3300
¹² C	²⁰⁸ Pb	35	11.30	1.00	298		3894	3561
¹² C	²⁰⁸ Pb	40	11.30	1.00	287		3898	
¹² C	²⁰⁸ Pb	120	11.30	1.00	158		3629	3136
¹⁶ O	⁹⁰ Zr	94	13.58	1.00	190		2752	2749
¹⁶ O	²⁰⁸ Pb	94	14.85	1.00	192		3879	3485
⁴⁰ Ar	²⁰⁸ Pb	44	33.50	1.00	280		5017	

TABLE II: Values obtained for the diffuseness of the matter densities. The diffuseness indicated for the ${}^4\text{He}$ nucleus was obtained from the corresponding charge density. The root-mean-square radii of the matter (RMS_M) and charge (RMS_C) distributions are included in the table.

Nucleus	a (fm)	RMS_M (fm)	RMS_C (fm)
${}^4\text{He}$	≈ 0.3	1.68	1.68
${}^6\text{He}$	0.56	2.40	
${}^6\text{Li}$	0.56	2.40	2.55
${}^7\text{Li}$	0.54	2.38	2.39
${}^{12}\text{C}$	0.58	2.73	2.47
${}^{16}\text{O}$	0.59	2.90	2.74
${}^{28}\text{Si}$	0.59	3.27	3.10
${}^{40}\text{Ca}$	0.56	3.50	3.48
${}^{40}\text{Ar}$	0.56	3.50	3.41
${}^{58}\text{Ni}$	0.59	3.94	3.77
${}^{90}\text{Zr}$	0.56	4.42	4.26
${}^{208}\text{Pb}$	0.54	5.72	5.50